

Infrared transparent carbon nanotube thin films

Liangbing Hu,^{a)} David S. Hecht, and George Grüner

Department of Physics, University of California, Los Angeles, California 90095, USA

(Received 4 November 2008; accepted 21 December 2008; published online 24 February 2009)

We have measured the infrared properties of optically transparent and electrically conductive single walled carbon nanotube thin films. We found that nanotube films with sheet resistance values of 200 Ω /sq show outstanding transmittance in the infrared range up to at least 22 μm , with an average transmittance greater than 90% over this range. The infrared properties of various materials were compared and we found that transparent nanotube electrodes and transparent graphene electrodes outperform the others in several key categories. This study opens another important application area for conductive nanotube thin films. © 2009 American Institute of Physics.

[DOI: 10.1063/1.3075067]

Transparent and conductive electrodes are prevalent in optoelectronic devices including solar cells, solid state lighting, and displays. Conductive carbon nanotube (CNT) thin films, with their mechanical advantages, have been developed as a replacement for the traditionally used, but brittle, indium tin oxide (ITO).^{1–3} To date, studies of the optical properties of CNT thin films have focused on the visible range; detailed explorations of their infrared (IR) properties, especially in the mid- and far-IR range, are lacking. Further investigations into the IR spectral properties are necessary due to its importance to military and industrial applications such as IR imaging and sensing, IR emission devices, IR solar cells, and modulators for fiber communications.^{4–6} The major goal of this study is to study the IR optical properties of electrically conductive single-walled CNT thin films.

To measure the transmittance of single-walled CNT thin films in a broad wavelength range, glass and zinc selenide (ZnSe) substrates are used. Glass is transparent from the UV out to 2700 nm and ZnSe is transparent from the NIR out to approximately 22 μm . The combination of the two substrates allows measurements of the transmittance of CNT films from 200 nm to 22 μm , even for thin films that lack the structural integrity to be measured as free standing films. Thin films are desired because in thick free-standing films, the IR transmittance is limited due to high absorption.¹ The CNT film deposition method is detailed in our previous work.⁷ Briefly, laser CNTs were dispersed in water with surfactant and the dispersion was sprayed onto heated substrates. After deposition, the films were rinsed in water to remove excess surfactant. Typical films are 200 Ω /sq (OPS) with 80% transmittance at 550 nm. The calculated conductivity based on the formula cited in Ref. 2 is 1592 S/cm.² Fourier transform IR spectra show insignificant sodium dodecyl sulfate (SDS) residue in the films, indicating that the surfactant will not affect the transmittance measurement. Figures 1(a) and 1(b) show the transmittance of a glass substrate, a ZnSe substrate, and CNT thin films. CNT film transmittance was calculated as the total transmittance of film on substrate divided by the bare substrate transmittance. Several key features emerge. Most evident is that the CNT films maintain greater than $\sim 80\%$ transmittance over a wide wavelength range from 450 nm to 20 μm , at a sheet resis-

tance of 200 OPS. In the visible and NIR range, loss of transmittance is dominated by CNT interband absorption. As the wavelength increases from NIR out to 20 μm , film transmittance gradually decreases, as the wavelengths become comparable to the cutoff wavelength at the plasma edge (ω_p) and the films begin to reflect. The cutoff wavelength for CNT thin films is in the range of 10–25 μm , depending on the CNT doping level; more discussions will follow. Competition between absorption and reflection results in a transmittance peak around the 2500 nm range. Wu *et al.*¹ have previously measured the IR transmittance of CNT films up to 100 μm ; however, their measured transmittance was low due to the thickness (240 nm) of the free-standing films.

Above the IR window allowed by the ZnSe substrate, direct measurement of the IR properties of thin CNT films is difficult, due to the inevitable complications arising from the substrate. Therefore, to gain more insight into the IR properties of CNT thin films, especially the IR behavior above 20 μm , we used previously measured CNT optical constants to model the IR transmittance, reflection, and absorption of CNT films. We base our calculations on the optical constants reported by Ruzicka *et al.*⁸ from 400 nm to 2 cm. The pair of constants (σ_1, σ_2) allow us to calculate the other pairs (ϵ_1, ϵ_2) and (n, k) in any frequency or wavelength range. Based on (n, k), we are able to calculate the reflection, transmission, and absorption using a formula for electromagnetic radiation through thin films.⁹ The results for 30 nm thick films (sheet resistance ~ 200 OPS) are shown in Fig. 2. To check the accuracy of the calculation, the same calculation is applied for a 20 μm thick film and the result compared with the data published in paper of Degiorgi.⁸ The excellent agreement between our calculation and their measurement

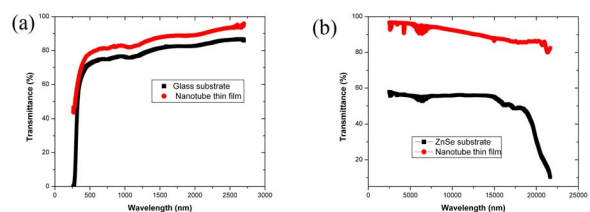


FIG. 1. (Color online) (a) Transmittance of glass substrate and a nanotube thin film from 250 to 2700 nm. (b) Transmittance of ZnSe substrate and a nanotube thin film from 2500 to 22000 nm.

^{a)}Electronic mail: hlb@physics.ucla.edu.

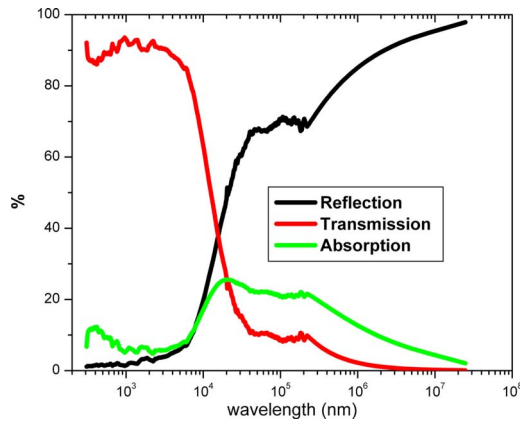


FIG. 2. (Color online) Calculation of reflection, transmittance, and absorption of nanotube thin films for a broad wavelength range from 400 nm to 2 cm. Film transmittance is high until reflection begins at wavelengths above the plasma wavelength.

prove the accuracy of our calculation. Considering the data in Fig. 2, one sees clear absorption peaks between 400 and 1000 nm, which are due to interband absorption. Moving toward the IR, Fig. 2 shows that the absorption decreases and the reflection begins to increase sharply around 10 μm , leading to a ω_p around 20 μm (0.06 eV), in broad agreement with Ref. 1. Of course, since ω_p scales with density as $\omega_p \sim \sqrt{n}$, nanotube sources, which have different charge carrier densities, will have different ω_p . Much of the research effort in traditional transparent conducting oxides (TCOs) focuses on modifying the doping level in order to achieve both a high dc conductivity and a high level of transparency over the desired range. However, the inevitable tradeoff between dc conductivity and ω_p limits the application of TCOs, particularly in the IR range. For example, the cutoff wavelength is 1.1 μm for a heavily doped ITO electrode with a charge carrier density of $10^{21}/\text{cm}^3$.¹⁰ Since $\sigma = ne\mu$, it is preferable to increase the mobility rather than the carrier density to achieve high quality transparent electrodes. For CNT electrodes, this would mean modifying parameters such as tube length or material purity.¹¹ Another interesting feature in Fig. 2 is from 20 to 200 μm . In this wavelength range, the absorption shows a broad flat peak, which is in agreement with optical conductivity measurement of Degiorgi and co-workers, and is likely due to the metallic CNTs. For metallic CNTs with chiralities other than (n,n) , there are “bandgaps” of ~ 20 meV due to curvature effects, and the absorption in

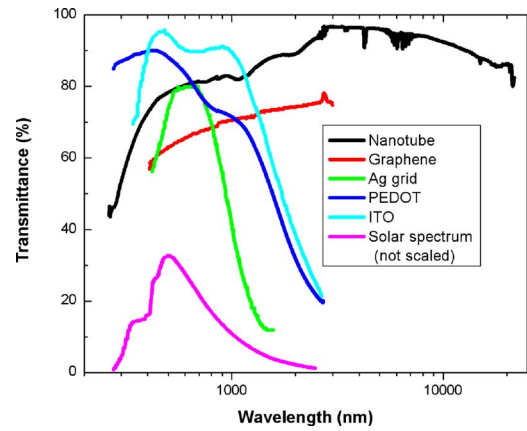


FIG. 3. (Color online) Comparison of spectra for various transparent and electrically conductive materials including nanotube thin film, graphene thin film, Ag nanowire thin film, PEDOT, and ITO to demonstrate the advantages of using nanotube and graphene thin films in the longer wavelength range.

this range is attributed to these small bandgap tubes. Above 200 μm , in the microwave frequency range and below, reflection is dominant due to the high conductance of our films. In this range, the reflection scales as $R \sim \log(fd)$ where f is frequency and d is the film thickness.¹⁰

Transparent electrodes are ubiquitous in optoelectronic device applications. TCOs are traditionally used, but there are several alternatives currently being developed including conductive polymers such as poly(3,4-ethylenedioxythiophene): poly(styrenesulfonate) (PEDOT: PSS), thin metal films, and random networks or thin films of conductive nanomaterials such as CNTs, graphene, and metal nanowires. Figure 3(a) summarizes the spectra of various transparent electrodes currently available in the literature, along with our measurement for a CNT thin film from Fig. 1.^{8,12–23} The transmittance for the transparent electrodes are typical data for given sheet resistance and process conditions, as listed in Table I. Graphene thin films are chemically similar to CNTs due to the fundamental chemical bonds and have been recently developed as an alternative for transparent and conductive electrodes. The spectrum for graphene in the visible and NIR is similar to that for CNTs. The transmission increases with increasing wavelength and no peak exists over the measurement range. Graphene has the same plasma energy as graphite, about 0.3 eV.²² Therefore, it is expected that a graphene thin film will remain transparent in the IR range up to ~ 4 μm wavelength. Additional optical

TABLE I. Comparison for various transparent electrodes.

	Thickness (nm)	R_s (Ω/S)	T at 550 nm (%)	Figure of merit T at 550 nm T^{10}/R_s	T at 3 μm (%)	Figure of merit T at 3 μm T^{10}/R_s	R at 550 nm (%)	A at 550 nm (%)	Conductivity (S/cm)	n (550 nm)	k (550 nm)	Carrier density (cm^{-3})	ω_p (Hz)	Cutoff wavelength	Refs.
Carbon nanotube	25	200	80	0.54	90	1.74	<1	8	2 000	1.03–1.5	0.24	10^{17} ^a	10^{13} ^b	10–20 μm	8 and 11–15
Graphene	10	1800	70	0.02	75	0.031	18	12	555	1.57	0.25	10^{18}	7×10^{13}	4 μm	16 and 17
Metal nanowire or thin film (i.e., Ag or Au)	Average 10 nm	22	88	12.66	10	4.5×10^{-9}	15	5	45 454	–	–	5.868×10^{22}	9×10^{14}	330 nm	18–21
PEDOT	50	200	85	0.98	20	5×10^{-7}	9	6	1 000	1.5	0.04–0.2	–	3×10^{14}	~ 1 μm	22
ITO	50–120	10–300 ^d	88	0.93–27.85	20	1×10^{-6}	12	0	~ 1 000 on plastic	2.0 ^e	0	$\sim 10^{20}$	2.8×10^{14}	~ 1 μm	9 and 18

^aThe numbers are calculated using the formula $\text{Conductivity} = \mu en$ for carbon nanotube.

^bThe numbers are calculated using the formula $m = 0.02m_e$ for carbon nanotube.

^cThe average thickness is calculated from the geometric aperture of 90% and nanowire height of 100 nm.

^dThe sheet resistance depends on substrate and process conditions.

^eMeasurement at 1.5 μm used.

properties of graphene thin films could be calculated based on existing optical conductivity data for graphite.¹⁷ Transparent electrodes consisting of a random or aligned network of metal nanowires has also been recently developed. Typically these metal nanowires have diameters ranging from 30–100 nm and cover approximately 10% of the surface; this leads to films with an effective thickness around 10 nm, and such films will remain transparent and highly electrically conductive. Although metal nanowires have lower charge carrier mobility than the bulk metal due to boundary scattering, the carrier density will remain the same as the bulk counterpart. Similar to networks of metal nanowires, patterned metal grids are emerging as a material that has possibilities as a transparent electrode. Metal grids should have an IR transmittance similar to metal nanowires.^{18–20} The major difference is that metal grids will have a larger grid size, higher mobility, and a more ordered structure than metal nanowire networks. Metal nanowire networks, metal grid, or thin metal films would share similar IR properties. The skin depth of metal such as silver is in the range of 10–20 nm at 550 nm wavelength; therefore thin metal or nanowire films are only transparent for films less than 10–20 nm. As the wavelength increases, the skin depth also increases, which causes a dramatic increase in the reflection. Therefore, thin metal or metal nanowire films have poor IR transmittance, as indicated in Fig. 3(a). The transmittance spectrum of conductive polymer PEDOT: PSS has an absorption peak at 400 nm. PEDOT: PSS has poor transmittance at wavelengths above 1 μm due to high reflection.²² For an ITO electrode, doping levels that lead to low sheet resistance also tend to shift the ω_p to $\sim 1 \mu\text{m}$, making them nontransparent in much of the IR.⁹ Figure 3(b) shows a plot of the visible and NIR spectra for the various transparent electrode materials considered here, overlay with the solar spectrum (not to scale). All materials shown have high transmittance in the visible and near IR range. However, above this range, the transmittance drops precipitously for all materials except for nanotube and graphene thin films, due to their lower carrier density. Since approximately 40% of the solar energy is above a wavelength of 1 μm , it is suggested here that for high efficiency solar cell applications, especially for IR solar cells, transparent nanotube and graphene thin films are promising materials.

Table I summarizes the electrical and optical properties of the discussed transparent electrodes. The data are either taken directly from references, or calculated based on standard equations for optical properties. Several things are apparent from the table. First, PEDOT, CNT, and graphene thin films have high work functions, which can be used as anodes in optoelectronic devices. Second, due to their low charge carrier density, CNT and graphene have high cutoff wavelengths, which make them appropriate for applications requiring IR transparent electrodes. CNT thin films have the highest cutoff wavelength, and are the best candidate for longer wave IR applications. Last, CNT thin films have the lowest reflection among the transparent films discussed here. Metal nanowires, graphene, and ITO all have reflection larger than 10% in the visible range, such that an antireflection coating is preferred for these electrodes. Table I provides a useful source for selecting transparent electrodes for different applications.

In conclusion, we have studied the IR properties of electrically conductive CNT thin films in a broad wavelength

range. We measured the spectra from 400 nm to 22 μm and compared these measurements with calculations based on data in the literature. CNT thin films show outstanding transmittance up to 22 μm wavelength. While this high IR transmittance makes CNT films a poor candidate for use as a heat blocking window, it proves useful for applications where heat dissipation is required. One example is for solar cells, where excess heat generated in the device can be dissipated through radiative IR transmission. Also, we compare the electrical and optical properties of various transparent electrodes and compared their materials properties. This analysis should provide a good source for people to choose transparent electrodes for various applications. For IR device applications, CNT and graphene thin films show substantial advantages over other transparent electrode, additionally, the spectra in this study for films with mixed metallic and semiconducting nanotubes. For separated nanotubes, ω_p will shift toward higher value for metallic tubes and shift toward lower value for semiconducting tubes due to the difference in carrier density. Although the absorption peaks will be different, which are mainly in the visible and NIR range,²⁴ the property of IR transparency for separated tubes will still apply due to the small thickness.

This work is supported by NSF Grant No. DMR-0404029.

¹Z. Wu, Z. Chen, X. Du, J. M. Logan, J. Sippel, M. Nikolou, K. Kamaras, J. R. Reynolds, D. B. Tanner, F. Hebard, and A. G. Rinzler, *Science* **305**, 1273 (2004).

²L. Hu, D. S. Hecht, and G. Gruner, *Nano Lett.* **4**, 2513 (2004).

³Q. Cao, S.-H. Hur, Z. Zhu, Y. Sun, C. Wang, M. Meitl, M. Shim, and J. A. Rogers, *Adv. Mater. (Weinheim, Ger.)* **18**, 304 (2006).

⁴G. Xu, Z. Liu, J. Ma, B. Liu, S. Ho, L. Wang, P. Zhu, T. Marks, J. Luo, and A. Jen, *Opt. Express* **13**, 7380 (2005).

⁵N. Shi Kam, M. O'Connell, J. Wisdom, and H. Dai, *Proc. Natl. Acad. Sci. U.S.A.* **102**, 11600 (2005).

⁶Y.-B. Park, L. Hu, G. Gruner, G. Irvin, and P. Drzaic, *SID Int. Symp. Digest Tech. Papers*, **37**, 537 (2008).

⁷L. Hu, G. Gruner, J. Gong, C. J. Kim, and B. Hornbostel, *Appl. Phys. Lett.* **90**, 093124 (2007).

⁸B. Ruzicka, L. Degiorgi, R. Gaal, L. Thien-Nga, R. Bacsa, J.-P. Salvetat, and L. Forro, *Phys. Rev. B* **61**, R2468 (2000).

⁹M. Dressel and G. Gruner, *Electrodynamics of Solids: Optical Properties of Electrons in Matter* (Cambridge University Press, Cambridge, 2002); T. Coutts, D. Young, and X. Li, *MRS Bull.* **25**, 58 (2004).

¹⁰H. Xu, S. Anlage, L. Hu, and G. Gruner, *Appl. Phys. Lett.* **90**, 183119 (2007).

¹¹D. S. Hecht, L. Hu, and G. Gruner, *Appl. Phys. Lett.* **89**, 133112 (2006).

¹²J. Li, L. Hu, L. Wang, Y. Zhou, G. Gruner, and T. Marks, *Nano Lett.* **6**, 2472 (2006).

¹³M. Barnes, J. van de Lagemaat, D. Levi, G. Rumbles, T. J. Coutts, C. L. Weeks, D. A. Britz, I. Levitsky, J. Peltola, and P. Glatkowski, *Phys. Rev. B* **75**, 235410 (2007).

¹⁴G. Fanchini, H. E. Unalan, and M. Chhowalla, *Appl. Phys. Lett.* **88**, 191919 (2006).

¹⁵G. Baumgartner, M. Carrard, L. Zuppiroli, W. Bacsa, W. A. de Heer, and L. Forro, *Phys. Rev. B* **55**, 6704 (1997).

¹⁶F. Wang, G. Dukovic, L. Brus, and T. Heinz, *Science* **308**, 838 (2005).

¹⁷E. A. Taft and H. R. Philipp, *Phys. Rev.* **138**, A197 (1965).

¹⁸X. Wang, L. Zhi, and K. Mullen, *Nano Lett.* **8**, 323 (2008).

¹⁹N. Lee, S. Connor, Y. Cui, and P. Peumans, *Nano Lett.* **8**, 689 (2008).

²⁰M. G. Kang, M. S. Kim, J. Kim, and L. Guo, *Adv. Mater. (Weinheim, Ger.)* **20**, A1 (2008).

²¹Data sheet from CPFilm Inc, www.cpfilm.com.

²²Y. Ha, N. Nikolov, S. Pollack, J. Mastrangelo, B. Martin, and R. Shashidhar, *Adv. Funct. Mater.* **14**, 615 (2004).

²³L. G. Johnson and G. Dresselhaus, *Phys. Rev. B* **7**, 2275 (1973).

²⁴A. Green and M. Hersam, *Nano Lett.* **8**, 1417 (2008).